Zha and Zhang
Chinese Journal of Mechanical Engineering (2024) 37:46
https://doi.org/10.1186/s10033-024-01028-2

Chinese Journal of Mechanical Engineering

ORIGINAL ARTICLE **Open Access**

Geometric Error Identification of Gantry-Type CNC Machine Tool Based on Multi-Station Synchronization Laser Tracers

Jun Zha[1,2*] and Huijie Zhang[1]

Abstract
Laser tracers are a three-dimensional coordinate measurement system that are widely used in industrial measurement. We propose a geometric error identification method based on multi-station synchronization laser tracers to enable the rapid and high-precision measurement of geometric errors for gantry-type computer numerical control (CNC) machine tools. This method also improves on the existing measurement efficiency issues in the single-base station measurement method and multi-base station time-sharing measurement method. We consider a three-axis gantry-type CNC machine tool, and the geometric error mathematical model is derived and established based on the combination of screw theory and a topological analysis of the machine kinematic chain. The four-station laser tracers position and measurement points are realized based on the multi-point positioning principle. A self-calibration algorithm is proposed for the coordinate calibration process of a laser tracer using the Levenberg–Marquardt nonlinear least squares method, and the geometric error is solved using Taylor's first-order linearization iteration. The experimental results show that the geometric error calculated based on this modeling method is comparable to the results from the Etalon laser tracer. For a volume of 800 mm × 1000 mm × 350 mm, the maximum differences of the linear, angular, and spatial position errors were 2.0 μm, 2.7 μrad, and 12.0 μm, respectively, which verifies the accuracy of the proposed algorithm. This research proposes a modeling method for the precise measurement of errors in machine tools, and the applied nature of this study also makes it relevant both to researchers and those in the industrial sector.

Keywords Multi-point positioning, Multi-station synchronization, CNC machine tool, Geometric error, Error separation

1 Introduction

Multi-point positioning technology is used to monitor the real-time dynamic information of a target at the airport and for aviation flight, management, and control. This technology uses the time taken for the moving target to reach the position of each receiving base station, and realizes the accuracy of the moving target based on the distance formula between two points [1]. The method to determine the geometric error measurement of computer numerical control (CNC) machine tools is based on the multi-point positioning principle and is realized using a laser tracking measurement system. This system is used to achieve the tracking measurement of the target point position. The measured length value is used to replace the arrival time and the positioning of the space target, and an accurate solution for the geometric error of the CNC machine tool is realized based on the distance formula between two points.

*Correspondence:
Jun Zha
jun_zha@xjtu.edu.cn
[1] School of Mechanical Engineering, Xi'an Jiaotong University, Xi'an 710049, China
[2] Xi'an Jiaotong University Suzhou Academy, Suzhou 215123, China

Laser tracking is used as a three-dimensional space coordinate measurement system. In recent years, it has been widely used in robot calibration [2], CNC machine tools and their component accuracy detection [3], large scene three-dimensional measurement, and large component assembly [4]. The methods used by laser tracking systems for the geometric error measurement of CNC machine tools are mainly divided into single-base station measurement methods, multi-base station time-sharing measurement methods, and multi-base station measurement methods. Schwenke et al. [5] used a single-station Etalon laser tracking interferometer to complete the geometric error separation of a five-axis CNC machine tool turntable and linear axis dynamic measurement. Fu et al. [6] used the single-base station measurement method to implement verticality error detection and circular trajectory tests for CNC machine tools. Wang et al. [7] proposed the concept of the multi-station time-sharing measurement and used a single laser tracker to complete the measurement of 21 geometric errors of a three-axis CNC milling machine within 4 h. Zhang et al. [8] used this method to measure the geometric error of a turntable, which was similar to the measurement result obtained by a ball bar. They then measured the geometric error of a linear guide platform [9], which was similar to the measurement result by a laser interferometer, which proved the effectiveness of this method. Li et al. [10] used this method to realize the pose measurement of the geometric error of CNC machine tools, and the calculated positioning error was closer to the measurement result obtained by a laser interferometer. Camboulives et al. [11] used the multi-base station method to conduct a three-dimensional space error correction of a coordinate measuring machine, and analyzed the measurement uncertainty of the multilateral measurement method. Gomez-Acedo [12] and Ibaraki [13] conducted a thermal error test of a three-axis CNC machine tool and the thermal deformation analysis of the space trajectory, respectively. Lee et al. [14] completed the identification of the servo mismatch error of CNC machine tools based on the circle test, which expanded the application range of the laser tracking measurement system. Therefore, it is clear that the single-base station method and multi-base station time-sharing measurement method are currently widely used in the above-mentioned research.

The multi-base station time-sharing measurement method and the single-base station measurement method are used to realize the coordinate measurement of the target point position based on the multi-point positioning principle. The coordinates of any point in the selected space are solved according to the positions of three or more base stations in that space. The important aspect of these two methods is to realize the base station self-calibration and measuring point algorithm, one of which is solved in the tracker's own coordinate system, and the other is solved in the machine coordinate system. Most previous studies have realized self-calibration and the measuring point algorithm based on the multi-base station time-sharing measurement method, and they have used translation and rotation transformations to convert self-calibration and machine tool coordinate systems during the solution process. Lin et al. [15] and Takatsuji et al. [16] used this method to implement the base station self-calibration and measurement algorithm. The single-base station measurement method uses the theoretical point coordinates of the machine tool for self-calibration in the machine tool coordinate system, which can directly realize the identification of the geometric error in this coordinate system. However, the measurement process easily introduces the spatial position error of the CNC machine tool itself and is influenced by repeated positioning accuracy. This reduces the calibration accuracy of the base station, which results in inaccurate measurement results.

Although this effect can be ignored for non-precision machine tools, it is still a source of large errors, which greatly limits the scope of application of this method. Song et al. [17] discussed the measurement principle of a laser tracker and used the theoretical coordinates of the machine tool to calibrate the laser tracker. They then used the calibrated base station position coordinates to calculate the space measurement point coordinates and separated and obtained the geometric errors of CNC machine tools. Previously, Wang et al. [7] used the least squares method to achieve the theoretical solution of this method. Chen et al. [18] used singular value decomposition to achieve rapid separation of geometric errors and avoid the singularity of the solution. Wan et al. [19] optimized the self-calibration and measurement point algorithm using a Gaussian random distribution. In addition, Wendt et al. [20] used an additional condition constraint method to detect the spatial error of a large three-coordinate measuring machine using a four-base station tracker in the machine tool coordinate system. Schwenke et al. [21] used a single-station laser tracking interferometer to detect the geometric errors of a three-coordinate measuring machine using the additional constraint method. The calculated result is similar to that acquired by the ball-plate method, thereby verifying the correctness of the method and analyzing the measurement uncertainty degree. The additional constraint method has a higher calculation accuracy, and it is suitable for situations with more constraints in the solution; however, the calculation efficiency requires improvement. Li et al. [22] introduced a precision turntable coordinate system to measure the geometric error of a single linear axis and turntable. This method avoided the use of machine tool and tracker coordinate systems. However, the additional device increases the measurement cost and difficulty, and the conversion relationship between coordinate systems is not discussed; thus, there are still major limitations. To mitigate this limitation, Zha et al. [23] used a four-station laser tracers to measure the geometric error of the precision turntable. While ensuring measurement accuracy, the measurement speed was increased by four times.

A relative length measurement using laser interference does not require an accurate angle measurement by the tracker, and it is sufficient to track the target position. The relative length is set as an accurate value in the solution algorithm, and the dead zone length must be solved [24]. There is no influence from the dead zone length during use; however, it needs to be accurately calculated from the angular positioning. Moreover, the absolute length measurement accuracy of the tracker is weaker than the relative length measurement accuracy. Therefore, the source of the geometric error of the three-axis gantry structure CNC machine tool was analyzed, and a geometric error mathematical model was established using screw theory. Additionally, the laser tracer position self-calibration was realized based on the Levenberg–Marquardt nonlinear least square method, and the geometric error separation was realized. Geometric error items and spatial position errors were obtained from experimental measurements, and they were compared with the calculated results of the laser tracer to verify the correctness of the measurement algorithm.

2 Geometric Error Analysis

The geometric error is the inherent error of CNC machine tools [25, 26], and its main source is the change in geometric parameters caused by the machining quality of CNC machine tool parts and the change in the relative position relationship caused by factors such as parts assembly. Assuming that the axis of motion is an ideal rigid body, there is a deviation of six degrees of freedom in space during a single-axis motion, i.e., the deviation of position and attitude.

Taking the linear axis of motion Y as an example, its pose deviation is $P_{\mathrm{Y}} = [E_{\mathrm{XY}}, E_{\mathrm{YY}}, E_{\mathrm{ZY}}, E_{\mathrm{AY}}, E_{\mathrm{BY}}, E_{\mathrm{CY}}]^{\mathrm{T}}$, as shown in Figure 1. In this formula, E_{XY} is the straightness error of the Y-axis along the X-direction, E_{YY} is the Y-axis positioning error, E_{ZY} is the straightness error of the Y-axis along the Z-axis, E_{AY} is the pitch error of the Y-axis, E_{BY} is the roll error, and E_{CY} is the Y-axis yaw error.

The six geometric errors of a single axis are all position-related errors, and the relative position changes caused by the assembly between the axes are position-unrelated errors, such as verticality errors [27]. Therefore, there are

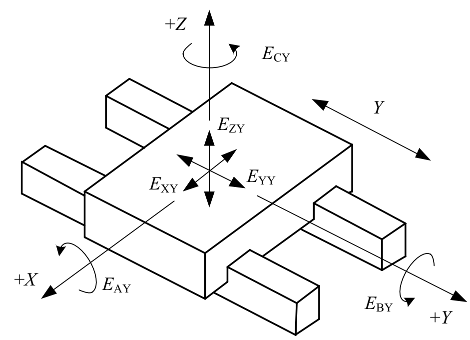

Figure 1 Geometric error terms of *Y*-axis

21 geometric errors in the three-axis CNC machine tool, and the error terms are shown in Table 1. In the process of the geometric error modeling of a three-axis gantry CNC machine tool, the machine tool coordinate system is used after the X-, Y-, and Z-axes are zeroed. The machine tool coordinate system is set as the base coordinate system, and to facilitate subsequent geometric error modeling, all geometric errors are defined in this coordinate system.

3 Geometric Error Modeling

The kinematic chain of the three-axis gantry structure CNC machine tool, from the workpiece to the tool, is W-F-Y-X-Z-T (W is the workpiece, F is the bed representing the base coordinate system, and T is the tool). The kinematic chain is shown in Figure 2(a), and the actual machine tool is shown in Figure 2(b). First, we establish the tool coordinate system, which is the end coordinate system and the base coordinate system. The base coordinate system used here is the bed coordinate system. When analyzing 21 geometric errors in the space of a three-axis gantry CNC machine tool, all motion axes return to zero to their initial positions. At this time, the base coordinate system coincides with the tool coordinate system and is consistent with the machine tool coordinate system; the zero point is set as the reference point. In addition, in the non-processing state, the workpiece can be considered to be consistent with the base coordinate system during the measurement process. Thus, geometric error modeling can be conducted according to screw theory [28].

All geometric error terms are expressed in the basic coordinate system, and each error term is simplified according to the small displacement screw. Chasles' theorem states that any rigid body motion can be described using the superposition of the rotational and translational motions around the unit axis. Taking the Y-axis as an example, the geometric error modeling process based on screw theory is as follows.

Table 1 Geometric error terms of three-axis gantry-type machine tool

Linear axis and error classification		X	Y	Z
Position-related geometric error	Positioning error	E_{XX}	E_{YY}	E_{ZZ}
	Straightness error	E_{YX}, E_{ZX}	E_{XY}, E_{ZY}	E_{XZ}, E_{YZ}
	Angle error	E_{AX}, E_{BX}, E_{CX}	E_{AY}, E_{BY}, E_{CY}	E_{AZ}, E_{BZ}, E_{CZ}
Position-unrelated geometric error	Squareness error	E_{C0Y}	–	E_{A0Z}, E_{B0Z}

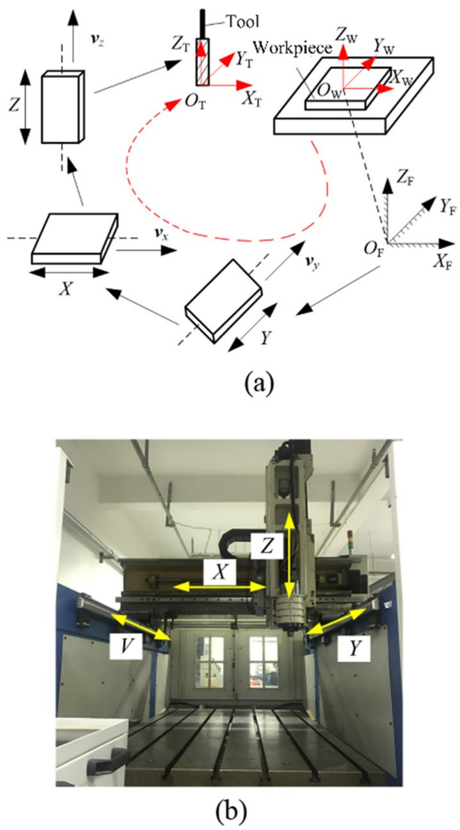

Figure 2 Three-axis gantry-type machine tool kinematic structure: (**a**) Chain diagram, (**b**) Physical photograph

The Y-axis geometric error motion pose can be described by the following equation:

$$g_{FY}^{e}(\boldsymbol{\theta}) = e^{\hat{\xi}_y\theta_y} e^{\hat{\xi}_{E_{YY}}\theta_{E_{YY}}} e^{\hat{\xi}_{E_{XY}}\theta_{E_{XY}}} e^{\hat{\xi}_{E_{ZY}}\theta_{E_{ZY}}} e^{\hat{\xi}_{E_{AY}}\theta_{E_{AY}}} e^{\hat{\xi}_{E_{BY}}\theta_{E_{BY}}} e^{\hat{\xi}_{E_{CY}}\theta_{E_{CY}}} \boldsymbol{g}_{FY}(\mathbf{0}). \tag{1}$$

In Eq. (1), the theoretical geometric error modeling parameters of the spinor can be selected and calculated, as shown in Table 2. The $\boldsymbol{g}_{FY}(\mathbf{0})$ is the initial pose, as shown in Eq. (2), and the target mirror is placed at the origin of the end coordinate system. Any rotational motion in three-dimensional space can be described as a rotation around a particular unit axis $\boldsymbol{\omega}=[\omega_1, \omega_2, \omega_3]^{\mathrm{T}}$. If the rotation angle is set to θ, $\boldsymbol{q}$ is the coordinate of any point on the rotation axis, and $\boldsymbol{v}$ is the direction of motion of the linear axis.

$$\boldsymbol{g}_{FY}(\mathbf{0}) = \begin{bmatrix} 1\,0\,0\,0 \\ 0\,1\,0\,0 \\ 0\,0\,1\,0 \\ 0\,0\,0\,1 \end{bmatrix}. \tag{2}$$

Using the exponential product formula, the kinematic model in Eq. (2) can be simplified into matrix form:

$$g_{FY}^{e}(\boldsymbol{\theta}) = \begin{bmatrix} 1 & -E_{CY} & E_{BY} & E_{XY} \\ E_{CY} & 1 & -E_{AY} & \mathrm{Y}+E_{YY} \\ -E_{BY} & E_{AY} & 1 & E_{ZY} \\ 0 & 0 & 0 & 1 \end{bmatrix}. \tag{3}$$

The theoretical geometric error modeling parameters of the squareness error screw are shown in Table 3.

Table 2 Screw parameters of *Y*-axis geometric error

Y	$e^{\hat{\xi}_y\theta_y}$	$e^{\hat{\xi}_{E_{YY}}\theta_{E_{YY}}}$	$e^{\hat{\xi}_{E_{XY}}\theta_{E_{XY}}}$	$e^{\hat{\xi}_{E_{ZY}}\theta_{E_{ZY}}}$	$e^{\hat{\xi}_{E_{AY}}\theta_{E_{AY}}}$	$e^{\hat{\xi}_{E_{BY}}\theta_{E_{BY}}}$	$e^{\hat{\xi}_{E_{CY}}\theta_{E_{CY}}}$
$\boldsymbol{\omega}$	–	–	–	–	$[1\ 0\ 0]^{\mathrm{T}}$	$[0\ 1\ 0]^{\mathrm{T}}$	$[0\ 0\ 1]^{\mathrm{T}}$
$\boldsymbol{q}$	–	–	–	–	$[0\ 0\ 0]^{\mathrm{T}}$	$[0\ 0\ 0]^{\mathrm{T}}$	$[0\ 0\ 0]^{\mathrm{T}}$
$\boldsymbol{v}$	$[0\ 1\ 0]^{\mathrm{T}}$	$[0\ 1\ 0]^{\mathrm{T}}$	$[1\ 0\ 0]^{\mathrm{T}}$	$[0\ 0\ 1]^{\mathrm{T}}$	$[0\ 0\ 0]^{\mathrm{T}}$	$[0\ 0\ 0]^{\mathrm{T}}$	$[0\ 0\ 0]^{\mathrm{T}}$
θ	Y	E_{YY}	E_{XY}	E_{ZY}	E_{AY}	E_{BY}	E_{CY}

Table 3 Screw parameters of squareness error

Y	$e^{\hat{\xi}_{E_{C0X}}\theta_{E_{C0X}}}$	$e^{\hat{\xi}_{E_{A0Z}}\theta_{E_{A0Z}}}$	$e^{\hat{\xi}_{E_{B0Z}}\theta_{E_{B0Z}}}$
ω	$[0\ 0\ 1]^T$	$[1\ 0\ 0]^T$	$[0\ 1\ 0]^T$
q	$[0\ 0\ 0]^T$	$[0\ 0\ 0]^T$	$[0\ 0\ 0]^T$
v	$[0\ 0\ 0]^T$	$[0\ 0\ 0]^T$	$[0\ 0\ 0]^T$
θ	E_{C0X}	E_{A0Z}	E_{B0Z}

Therefore, the kinematics formula of the three-axis gantry CNC machine tool based on screw theory, including geometric errors, can be expressed as:

$$\begin{aligned} g_{FT}^{e}(\theta) = {} & e^{\hat{\xi}_y\theta_y} e^{\hat{\xi}_{E_{YY}}\theta_{E_{YY}}} e^{\hat{\xi}_{E_{XY}}\theta_{E_{XY}}} e^{\hat{\xi}_{E_{ZY}}\theta_{E_{ZY}}} e^{\hat{\xi}_{E_{AY}}\theta_{E_{AY}}} e^{\hat{\xi}_{E_{BY}}\theta_{E_{BY}}} \\ & e^{\hat{\xi}_{E_{CY}}\theta_{E_{CY}}} e^{\hat{\xi}_{E_{C0X}}\theta_{E_{C0X}}} e^{\hat{\xi}_x\theta_x} e^{\hat{\xi}_{E_{XX}}\theta_{E_{XX}}} e^{\hat{\xi}_{E_{YX}}\theta_{E_{YX}}} e^{\hat{\xi}_{E_{ZX}}\theta_{E_{ZX}}} e^{\hat{\xi}_{E_{AX}}\theta_{E_{AX}}} \\ & e^{\hat{\xi}_{E_{BX}}\theta_{E_{BX}}} e^{\hat{\xi}_{E_{CX}}\theta_{E_{CX}}} e^{\hat{\xi}_{E_{A0Z}}\theta_{E_{A0Z}}} e^{\hat{\xi}_{E_{B0Z}}\theta_{E_{B0Z}}} e^{\hat{\xi}_z\theta_z} e^{\hat{\xi}_{E_{ZZ}}\theta_{E_{ZZ}}} e^{\hat{\xi}_{E_{XZ}}\theta_{E_{XZ}}} \\ & e^{\hat{\xi}_{E_{YZ}}\theta_{E_{YZ}}} e^{\hat{\xi}_{E_{AZ}}\theta_{E_{AZ}}} e^{\hat{\xi}_{E_{BZ}}\theta_{E_{BZ}}} e^{\hat{\xi}_{E_{CZ}}\theta_{E_{CZ}}} g_{FT}(\mathbf{0}). \end{aligned} \tag{4}$$

In this equation, θ_x, θ_y, and θ_z represent the amount of movement of each linear axis, which can be represented by X, Y, and Z, respectively.

The geometric error pose and rotation parameters of the X- and Z-axis are shown in Tables 4 and 5, respectively.

In addition, A is the initial pose of the tool end. When only 17 geometric errors are considered and the end is the origin of the tool coordinate system, the calculation method is:

$$g_{FT}(\mathbf{0}) = \begin{bmatrix} 1&0&0&0\\0&1&0&0\\0&0&1&0\\0&0&0&1 \end{bmatrix}. \tag{5}$$

The difference between the actual pose and the ideal pose of a three-axis gantry CNC machine tool is the geometric error model:

$$\boldsymbol{\Delta}_{xyz} = g_{FT}^{e}(\theta) - g_{FT}^{a}(\theta) = \begin{bmatrix} \Delta \boldsymbol{R}_M^e & \Delta \boldsymbol{T}_M^e \\ \mathbf{0} & 1 \end{bmatrix}, \tag{6}$$

where $g_{FT}^{a}(\theta)$ is the ideal pose of the tool end. The calculation is shown in Eq. (7):

$$g_{FT}^{a}(\theta) = e^{\hat{\xi}_y\theta_y} e^{\hat{\xi}_x\theta_x} e^{\hat{\xi}_z\theta_z} g_{FT}(\mathbf{0}), \tag{7}$$

where $\Delta \boldsymbol{R}_M^e$ is the attitude error model and $\Delta \boldsymbol{T}_M^e$ is the spatial position error of a three-axis gantry structure CNC machine tool model. Using the screw parameters of the geometric error pose modeling of the three-axis gantry CNC machine tool, combined with exponential product matrix conversion, the attitude error and

Table 4 Screw parameters of *X*-axis geometric error

X	$e^{\hat{\xi}_x\theta_x}$	$e^{\hat{\xi}_{E_{XX}}\theta_{E_{XX}}}$	$e^{\hat{\xi}_{E_{YX}}\theta_{E_{YX}}}$	$e^{\hat{\xi}_{E_{ZX}}\theta_{E_{ZX}}}$	$e^{\hat{\xi}_{E_{AX}}\theta_{E_{AX}}}$	$e^{\hat{\xi}_{E_{BX}}\theta_{E_{BX}}}$	$e^{\hat{\xi}_{E_{CX}}\theta_{E_{CX}}}$
ω	–	–	–	–	$[1\ 0\ 0]^T$	$[0\ 1\ 0]^T$	$[0\ 0\ 1]^T$
q	–	–	–	–	$[0\ 0\ 0]^T$	$[0\ 0\ 0]^T$	$[0\ 0\ 0]^T$
v	$[1\ 0\ 0]^T$	$[1\ 0\ 0]^T$	$[0\ 1\ 0]^T$	$[0\ 0\ 1]^T$	$[0\ 0\ 0]^T$	$[0\ 0\ 0]^T$	$[0\ 0\ 0]^T$
θ	X	E_{XX}	E_{YX}	E_{ZX}	E_{AX}	E_{BX}	E_{CX}

Table 5 Screw parameters of *Z*-axis geometric error

Z	$e^{\hat{\xi}_z\theta_z}$	$e^{\hat{\xi}_{E_{ZZ}}\theta_{E_{ZZ}}}$	$e^{\hat{\xi}_{E_{XZ}}\theta_{E_{XZ}}}$	$e^{\hat{\xi}_{E_{YZ}}\theta_{E_{YZ}}}$	$e^{\hat{\xi}_{E_{AZ}}\theta_{E_{AZ}}}$	$e^{\hat{\xi}_{E_{BZ}}\theta_{E_{BZ}}}$	$e^{\hat{\xi}_{E_{CZ}}\theta_{E_{CZ}}}$
ω	–	–	–	–	$[1\ 0\ 0]^T$	$[0\ 1\ 0]^T$	$[0\ 0\ 1]^T$
q	–	–	–	–	$[0\ 0\ 0]^T$	$[0\ 0\ 0]^T$	$[0\ 0\ 0]^T$
v	$[0\ 0\ 1]^T$	$[0\ 0\ 1]^T$	$[1\ 0\ 0]^T$	$[0\ 1\ 0]^T$	$[0\ 0\ 0]^T$	$[0\ 0\ 0]^T$	$[0\ 0\ 0]^T$
θ	Z	E_{ZZ}	E_{XZ}	E_{YZ}	E_{AZ}	E_{BZ}	E_{CZ}

spatial position error of the measurement point after the geometric error modeling can be obtained. Because the four-station laser tracers are used for simultaneous measurement, it is assumed that the center of the target mirror is very close to the center of the spindle end face of the machine tool, i.e., there is no attitude deviation at the center of the tool coordinate system. By substituting the initial pose, as shown in Eq. (5), and simplifying, a geometric error model of CNC machine tools that contains only 17 geometric errors can be obtained.

$$\Delta \boldsymbol{R}_M^e = \begin{bmatrix} 0 & -E_{\mathrm{CX}} - E_{\mathrm{CY}} - E_{\mathrm{CZ}} & E_{\mathrm{BX}} + E_{\mathrm{BY}} + E_{\mathrm{BZ}} \\ E_{\mathrm{CX}} + E_{\mathrm{CY}} + E_{\mathrm{CZ}} & 0 & -E_{\mathrm{AX}} - E_{\mathrm{AY}} - E_{\mathrm{AZ}} \\ -E_{\mathrm{BX}} - E_{\mathrm{BY}} - E_{\mathrm{BZ}} & E_{\mathrm{AX}} + E_{\mathrm{AY}} + E_{\mathrm{AZ}} & 0 \end{bmatrix}, \tag{8}$$

$$\Delta \boldsymbol{T}_M^e = \begin{bmatrix} \Delta X \\ \Delta Y \\ \Delta Z \end{bmatrix} = \begin{bmatrix} E_{\mathrm{XX}} + E_{\mathrm{XY}} + E_{\mathrm{XZ}} + Z(E_{\mathrm{B0Z}} + E_{\mathrm{BX}} + E_{\mathrm{BY}}) \\ E_{\mathrm{YX}} + E_{\mathrm{YY}} + E_{\mathrm{YZ}} - Z(E_{\mathrm{A0Z}} + E_{\mathrm{AX}} + E_{\mathrm{AY}}) + X(E_{\mathrm{C0Y}} + E_{\mathrm{CY}}) \\ E_{\mathrm{ZX}} + E_{\mathrm{ZY}} + E_{\mathrm{ZZ}} - X \cdot E_{\mathrm{BY}} \end{bmatrix}. \tag{9}$$

The above error model is expressed in the form of matrix multiplication as follows:

$$\begin{bmatrix} \Delta X \\ \Delta Y \\ \Delta Z \end{bmatrix} = \begin{bmatrix} 1 & 0 & 0 & 0 & Z & 1 & 0 & 0 & 0 & Z & 0 & 1 & 0 & 0 & 0 & -Z & 0 \\ 0 & 1 & 0 & 0 & 0 & 0 & 1 & 0 & -Z & 0 & X & 0 & 1 & 0 & -X & 0 & -Z \\ 0 & 0 & 1 & 0 & 0 & 0 & 0 & 1 & 0 & -X & 0 & 0 & 0 & 1 & 0 & 0 & 0 \end{bmatrix} \cdot \begin{bmatrix} E_{\mathrm{XX}} \\ \vdots \\ E_{\mathrm{A0Z}} \end{bmatrix}. \tag{10}$$

The above matrix is simplified to:

$$\boldsymbol{E} = \boldsymbol{C} \cdot \boldsymbol{P}, \tag{11}$$

where $\boldsymbol{E}$ is the spatial position error, which is related to the number of selected CNC machine coordinates, $\boldsymbol{C}$ is the geometric error model coefficient matrix, and $\boldsymbol{P}$ is the 17 geometric errors.

4 Laser Tracer Position and Measuring Point Coordinate Calibration

By setting the sphere center of the laser tracer LT1 to the zero point of the coordinate system by self-calibrating the coordinate system, the sphere center of the laser tracer LT2 is positioned on the XL axis of the coordinate system, and that of LT3 is placed in the XLYL plane, the sphere center of the laser tracer LT4 is placed at a position that is not coplanar with the centers of the other three tracking interferometers. The calibration of the laser tracer and measurement points is realized by using the spatial points in the CNC machine tool.

The self-calibration algorithm is used to determine the mutual position relationship between the base stations, which is the core of the laser tracer position calibration and the subsequent measurement point algorithm. The Levenberg–Marquardt nonlinear least squares method is used to realize the optimization iterative solution of the self-calibrated position parameters of the laser tracer. In the self-calibrated coordinate system, it is assumed that there are m laser tracer stations to measure n target points in space. Suppose the distance from the ith laser-tracking interferometer to the jth measuring point for laser interferometric ranging is l_{ij}, where $j=1, 2, ..., n$. Additionally, because the laser interferometer is an absolutely accurate relative measurement, and the absolute measured length is not accurate, there is a dead zone length l_i ($i=1, 2, ..., m$) in the solution process. Therefore, the coordinates of the ith measuring station are the algebraic form of the measurement formula for the coordinates of the jth measuring point, as shown in Eq. (12). When the four-station laser tracers are used to measure the jth point, the formulas are shown in Eq. (13).

$$F_{ij} = \sqrt{\left(x_j^L - x_{pi}^L\right)^2 + \left(y_j^L - y_{pi}^L\right)^2 + \left(z_j^L - z_{pi}^L\right)^2} - (l_i + l_{ij}) = 0, \tag{12}$$

$$\begin{cases} \sqrt{\left(x_j^L - x_{p1}^L\right)^2 + \left(y_j^L - y_{p1}^L\right)^2 + \left(z_j^L - z_{p1}^L\right)^2} = l_1 + l_{1j}, \\ \sqrt{\left(x_j^L - x_{p2}^L\right)^2 + \left(y_j^L - y_{p2}^L\right)^2 + \left(z_j^L - z_{p2}^L\right)^2} = l_2 + l_{2j}, \\ \sqrt{\left(x_j^L - x_{p3}^L\right)^2 + \left(y_j^L - y_{p3}^L\right)^2 + \left(z_j^L - z_{p3}^L\right)^2} = l_3 + l_{3j}, \\ \sqrt{\left(x_j^L - x_{p4}^L\right)^2 + \left(y_j^L - y_{p4}^L\right)^2 + \left(z_j^L - z_{p4}^L\right)^2} = l_4 + l_{4j}. \end{cases} \tag{13}$$

By linearizing Eq. (12) and ignoring the higher-order terms, we obtain:

$$v_{ij} = f_{ij0} + a_{ij}\delta x_j^L + b_{ij}\delta y_j^L + c_{ij}\delta z_j^L - a_{ij}\delta x_{pi}^L - b_{ij}\delta y_{pi}^L - c_{ij}\delta z_{pi}^L - \delta l_i - l_{ij} - l_{i0}, \tag{14}$$

$$\begin{cases} f_{ij0} = \sqrt{\left(x_{j0}^L - x_{pi0}^L\right)^2 + \left(y_{j0}^L - y_{pi0}^L\right)^2 + \left(z_{j0}^L - z_{pi0}^L\right)^2}, \\ a_{ij} = \dfrac{x_{j0}^L - x_{pi0}^L}{f_{ij0}}, \; b_{ij} = \dfrac{y_{j0}^L - y_{pi0}^L}{f_{ij0}}, \; c_{ij} = \dfrac{z_{j0}^L - z_{pi0}^L}{f_{ij0}}, \\ l_{ij} = f_{ij0} - l_{ij} - l_{i0}, \end{cases} \tag{15}$$

where $(x_{j0}^L, y_{j0}^L, z_{j0}^L)$ is the initial coordinate value of each measuring point, $(x_{pi0}^L, y_{pi0}^L, z_{pi0}^L)$ is the approximate value of the theoretical coordinate of the base station, l_{i0} is the approximate theoretical value of the dead zone length, and v_{ij} is the residual error of the equation.

When the four-station laser tracers are used for the measurement, $m=4$. When the number of equations is greater than the number of unknowns, the equation can be solved. That is, when the number of measurement points is sufficient, the self-calibration of the laser tracer position and the solution of the space point coordinates for calibration can be realized.

After satisfying the above solving conditions, the equation can be written in the following format:

$$\boldsymbol{V} = \boldsymbol{A} \cdot \boldsymbol{\delta X} - \boldsymbol{L}. \tag{16}$$

The self-calibration algorithm is implemented in the self-calibration coordinate system, and the following constraints on the location of the base station are given:

$$x_{p1}^L = 0 \; ; \; y_{p1}^L = 0 \; ; \; z_{p1}^L = 0 \; ; \; y_{p2}^L = 0 \; ; \; z_{p2}^L = 0 \; ; \; z_{p3}^L = 0. \tag{17}$$

Therefore, matrix $\boldsymbol{A}$ needs to be transformed. The column coefficients corresponding to the above parameters in matrix $\boldsymbol{A}$ are all set to zero, and the transformed matrix is set to $\boldsymbol{A}_g$. In addition, the initial value of the above parameters must be set to zero in the calculation process to completely apply the constraints of the self-calibrating coordinate system on the six parameters.

Using the least square method under the same precision measurement conditions, the normal equations of the linearized equations can be obtained:

$$\left(\boldsymbol{A}_g^{\mathrm{T}}\boldsymbol{A}_g\right) \cdot \boldsymbol{\delta X} = \boldsymbol{A}_g^{\mathrm{T}}\boldsymbol{L}. \tag{18}$$

Here, the Levenberg–Marquardt method is used to introduce an optimization method using the relaxation factor μ to iteratively solve the nonlinear equations. A reasonable choice of the μ value can bring the solution process closer to the Gauss–Newton method or the steepest descent method to avoid falling into a local solution.

$$\boldsymbol{\delta X}=\left(\boldsymbol{A}_g^{\mathrm{T}}\boldsymbol{A}_g+\boldsymbol{\mu I}\right)^{-1} \cdot \left(\boldsymbol{A}_g^{\mathrm{T}}\boldsymbol{L}\right). \tag{19}$$

Through repeated iterations, we can obtain the position parameters of the laser tracer and the space point coordinates used for calibration. The iteration steps of the Levenberg–Marquardt nonlinear least squares method are as follows:

(1) The given initial values include: $\boldsymbol{d}_0 = [x_{pi0}, y_{pi0}, z_{pi0}, x_i, y_i, z_i, l_{i0}]^{\mathrm{T}}$, iteration judgment accuracy ε, given maximum number of iterations p, initial number of iterations $h{:}=0$, $\mu_0 = 10^{-3}$, $\nu = 5$, nonlinear equations $\boldsymbol{F}(\boldsymbol{d}) = 0$, $\varepsilon_0 = \|\boldsymbol{F}(\boldsymbol{d}_0)\|$.
(2) Solve for $\boldsymbol{\delta X}_h = -\left(\boldsymbol{A}_{gh}^{\mathrm{T}}\boldsymbol{A}_{gh} + \mu_h\boldsymbol{I}\right)^{-1}\boldsymbol{A}_{gh}^{\mathrm{T}}\boldsymbol{L}_h$, μ_h is the relaxation factor.
(3) If $h{:} \geq p$, stop and obtain $\boldsymbol{d}$.
(4) If $\|\boldsymbol{F}_h(\boldsymbol{d}_h)\| \leq \varepsilon_h$, $\boldsymbol{d}_{h+1} = \boldsymbol{d}_h + \boldsymbol{\delta X}_h$. If $\|\boldsymbol{\delta X}_h\| \leq \varepsilon$, stop and output $\boldsymbol{d}$, otherwise $\mu_{h+1} = \mu_h/\nu$, $h := h : +1$. Go to step 2. If $\|\boldsymbol{F}_h(\boldsymbol{d}_h)\| > \varepsilon_h$, let $\boldsymbol{d}_{h+1} = \boldsymbol{d}_h + \boldsymbol{\delta X}_h$. Resolve $\boldsymbol{\delta X}_h$ and return to step 1.

In the self-calibration method, plane points or spatial points can be used as measurement points in the self-calibration process to calculate the spatial position coordinates of the four-station laser tracers. The theoretical space position coordinates of each position coordinate system are known in the machine tool, and they are the given coordinate points in the machine tool motion trajectory. Therefore, when the calibration is completed, the measurement points in the self-calibrated coordinate system and the theoretical coordinate points in the machine tool coordinate system can be used to determine the coordinates of the measurement point and the laser tracer position from the self-calibrated coordinate system to the machine tool coordinate system based on the coordinate transform.

The geometric error measurement of a three-axis gantry CNC machine tool is performed by setting the origin of the machine coordinate system as the reference point. Therefore, the machine origin coordinates are first found in the self-calibrated coordinate system during coordinate transformation, and the translation matrix $\boldsymbol{T}_M$ is then calculated. The rotation matrix $\boldsymbol{R}_M$ is subsequently established, and its unknown quantities are α, β, and γ. After the rotation, the distance between each coordinate point and the corresponding point is the smallest in the machine tool coordinate system. Therefore, assuming that the point set is $\boldsymbol{P}_j$ in the self-calibrated coordinate system, and the point set is $\boldsymbol{Q}_j$

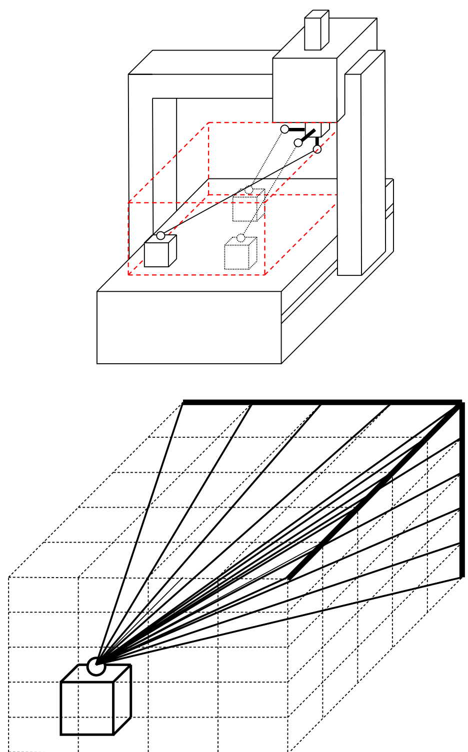

Figure 3 Schematic diagram showing the measurement of geometric errors of CNC machine tools by laser tracers

in the machine tool coordinate system, the objective function in the actual solution process is constructed as follows:

$$\boldsymbol{F}_M=\min\sum_{j=1}^{n}\left\|\boldsymbol{Q}_j-\left(\boldsymbol{R}_M\cdot\boldsymbol{P}_j+\boldsymbol{T}_M\right)\right\|^2, \tag{20}$$

where $\boldsymbol{R}_M$ is the rotation matrix between coordinate systems, $\boldsymbol{R}_M=\boldsymbol{R}_z(\gamma)\cdot\boldsymbol{R}_y(\beta)\ \boldsymbol{R}_x(\alpha)$; α, β, and γ are the rotation angles around the X-, Y-, and Z-axis, respectively, which are the waiting solved parameters in the objective function.

After the solution, the coordinates of the laser tracer and the calibration measuring point can be obtained in the machine tool coordinates. When the calibration of the measuring point is completed, the spatial position error of the target point can be calculated. The difference between the actual measured position coordinates and the theoretical coordinates is the spatial position error of the measuring point. This evaluation process requires only one measurement, and there is no need to determine the measurement point again after obtaining the position coordinates of the tracking interferometer in the machine coordinate system.

5 Geometric Error Separation in Gantry-Type CNC Machine Tool

The laser tracer measurement and geometric error solving algorithm are the key to realizing the rapid separation of geometric errors. This algorithm is solved based on the principle of multi-point positioning. The laser tracer quickly measures the spatial position error of CNC machine tools, as shown in Figure 3.

We assume m base stations (laser tracer here) and measure n measurement points. The measurement process can be expressed by the following nonlinear equation:

$$\boldsymbol{F}(\boldsymbol{d})=0, \tag{21}$$

where a particular nonlinear equation determines the difference between the length distance formula between two points when the ith laser tracer measures the jth target point. Additionally, the sum of the length of the laser tracer and the length of the dead zone is zero. The equation can be expressed as follows:

$$F_{ij}=\sqrt{\left(x_j-x_{pi}+\Delta x_j\right)^2+\left(y_j-y_{pi}+\Delta y_j\right)^2+\left(z_j-z_{pi}+\Delta z_j\right)^2}-\left(l_i+l_{ij}\right)=0. \tag{22}$$

In this equation, $\boldsymbol{d}$ is the unknown number in the solution, $\boldsymbol{d}=[x_{pj}, y_{pj}, z_{pj}, \boldsymbol{P}_j, l_i]^{\mathrm{T}}$; i is the ith laser tracer; $\boldsymbol{P}_j$ is all sets of geometric error terms at the jth measurement point; (x_j, y_j, z_j) is the theoretical coordinate value of the measuring point, and it is set to a known value according to the measurement track; (x_{pj}, y_{pj}, z_{pj}) is the position coordinate of the laser tracer to be solved; l_i is the length of the dead zone; $(\Delta x_{pj}, \Delta y_{pj}, \Delta z_{pj})$ is the spatial position error of the jth target measurement point, which can be calculated by the geometric error modeling formula.

The nonlinear least square Levenberg–Marquardt method is used to solve the above-mentioned nonlinear equations. This method can realize the least square solution of nonlinear small residual overdetermined equations, which is suitable for solving small residuals measured by a laser tracer and can avoid the shortcomings of the Gauss–Newton method falling into local solutions. Taylor expansion linearization is used to make a first-order approximation, and the nonlinear equations are written in matrix form as follows:

$$\boldsymbol{J}\cdot\boldsymbol{d}=\boldsymbol{F}'(\boldsymbol{d}), \tag{23}$$

where $\boldsymbol{J}$ is the Jacobian matrix of the nonlinear equation system, $\boldsymbol{F}'(\boldsymbol{d})$ is the substitute of the calculated value of each iteration into the $\boldsymbol{F}(\boldsymbol{d})$ value afterwards.

$$\boldsymbol{J}=\left[\frac{\partial F_{ij}(d)}{\partial d_k}\right]. \tag{24}$$

There are constraints according to the characteristics of various geometric errors: (1) The straightness is zero at the starting and end points of the solution; (2) all position-related errors are zero at the starting point. Therefore, all geometric error terms of a three-axis CNC machine tool have 12 constraints during the solution process. These 12 constraints are approximately the coordinate system of the agreed machine tool space. The settings are the same as the machine's inherent coordinate system, and the zero point is the reference point. These constraints can be expressed as a matrix:

$$\boldsymbol{B}\cdot\boldsymbol{P}=0, \tag{25}$$

where $\boldsymbol{B}$ is the constraint matrix that satisfies the constraint conditions and the matrix is full rank.

This constraint can be converted to:

$$\boldsymbol{B}'\cdot\boldsymbol{d}=0. \tag{26}$$

After integrating Eq. (23) and Eq. (26), the solution equation can be written as follows:

$$\boldsymbol{M}\cdot\boldsymbol{d}=\boldsymbol{G}, \tag{27}$$

where $\boldsymbol{M}$ is the coefficient matrix after the integration of linearized equations, $\boldsymbol{M}=[\boldsymbol{J},\boldsymbol{B}']^{\mathrm{T}}$, and $\boldsymbol{G}$ is the residual amount of the linearized equation after integration.

According to the above analysis and derivation, the calculation for each step of the Levenberg–Marquardt algorithm can be expressed using the following equation in the iterative solution process:

$$\boldsymbol{d}=-\left(\boldsymbol{M}^{\mathrm{T}}\boldsymbol{M}+\mu\boldsymbol{I}\right)^{-1}\boldsymbol{M}^{\mathrm{T}}\boldsymbol{G}. \tag{28}$$

After multiple Taylor first-order linearization iterative solutions, when the set solution accuracy and calculation times are met, 17 geometric errors for CNC machine tools can be obtained. When the four-station laser tracers are simultaneously measured, the frame or cross-shaped trajectory can be used to plan the geometric error measurement trajectory. The measurement of the spatial position error can be achieved by planning a single measurement. The measurement time is short, which can significantly reduce the influence of thermal errors in the measurement process. The entire measurement process takes approximately 0.5 h. When the four-station laser tracers make a measurement, each tracking interferometer measures the same trajectory. Therefore, the position coordinates of the measuring points can be accurately obtained, and the 17 geometric errors of the machine tool can be solved using this position coordinate information. In addition, to save measurement costs, when there is only a single laser tracer, the multi-base station time-sharing measurement method can be used to measure the geometric error of the CNC machine tool, and different trajectories can be planned for each base station location. However, it is required that at least three base stations can measure the position simultaneously in the planned trajectory and meet the necessary length measurement space intersection conditions to obtain the determined coordinates of the position.

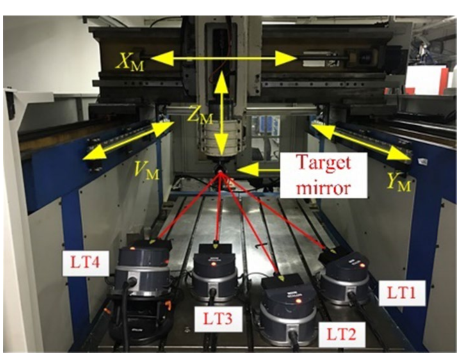

Figure 4 Three-axis gantry-type numerical control milling machine geometric error measurement

6 Experimental Verification

6.1 Geometric Error Comparison Experiment

In a standard temperature environment of 20 ± 2 °C, Etalon four-station laser tracers (Hexagon DEU01 GmbH, Series: LT00083-LT00086, Braunschweig, Germany) are

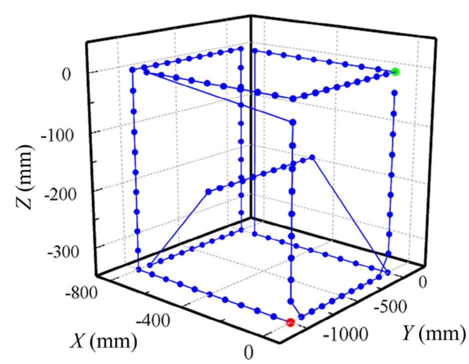

Figure 5 Three-axis gantry-type numerical control milling machine geometric error measurement trajectory

Table 6 Coordinates in the machine tool coordinate system after calibration of the four-station laser tracers

Laser tracer	X_P (mm)	Y_P (mm)	Z_P (mm)
LT_1	158.8075	−1456.6824	−349.7023
LT_2	−113.1165	−1671.7155	−349.3517
LT_3	−468.6489	−1563.1627	−349.4140
LT_4	−769.8987	−1599.5469	−208.9567

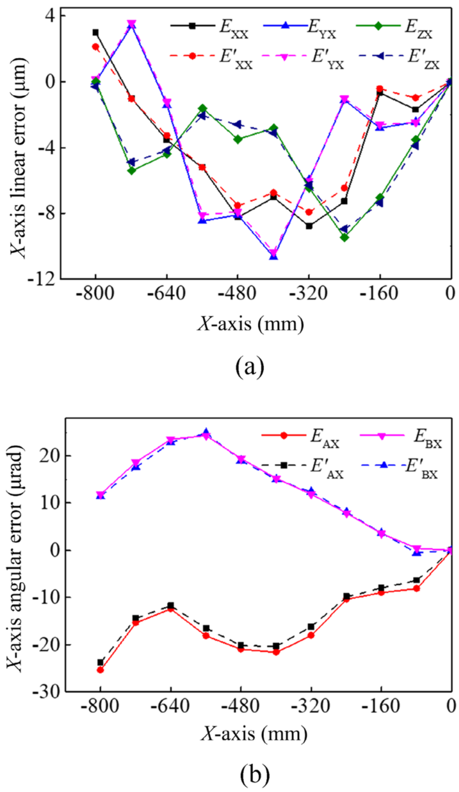

Figure 6 Comparison of *X*-axis geometric error measurement results: (**a**) Linear errors, (**b**) Angular errors of the *X*-axis

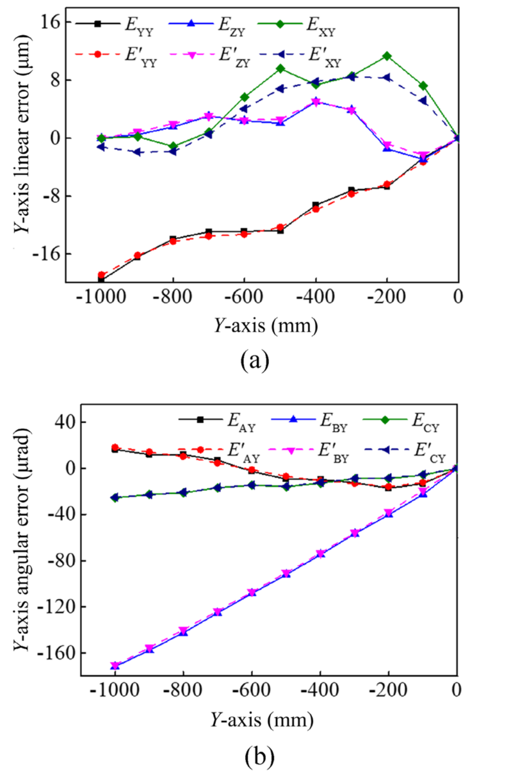

Figure 7 Comparison of *Y*-axis geometric error measurement results: (**a**) Linear errors, (**b**) Angular errors of the *Y*-axis

used to perform 17 geometric error measurement experiments on a three-axis gantry CNC milling machine. The measurement strokes of the *X*-, *Y*-, and *Z*-axis of the CNC machine tool are set to [−800 mm, 0], [−1000 mm, 0], and [−350 mm, 0], respectively, and the measurement trajectory is planned in the measurement space. The trajectory is required to cover the abovementioned measurement space. The trajectory planning steps on the *X*-, *Y*-, and *Z*-axes are 80 mm, 100 mm, and 35 mm, respectively, and 11 measurement points are selected on each axis. The measurement program is compiled according to the space target trajectory. In the program, the feed speed of the machine tool is set to 1000 mm/min, and the dwell time of each target position point is 3 s to ensure that the machine tool has a stable stopping time and the laser tracer has a sufficient data acquisition time. During the measurement process, a single two-way measurement is performed. The average round-trip length measurement of the same space target position made by the laser tracer is used as the measurement length result to be brought into the nonlinear equation system to solve the geometric error.

The measurement site and trajectory plan are shown in Figures 4 and 5, respectively. The trajectory meets the requirements of covering the entire measurement space.

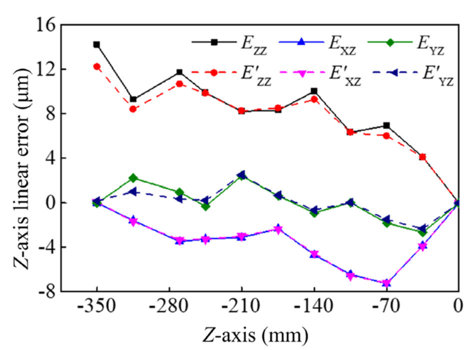

Figure 8 Comparison of *Z*-axis geometric errors measurement results

Table 7 Comparison of squareness error measurement results

Squareness error	E_{C0Y}	E_{B0Z}	E_{A0Z}
Self-editing algorithm (μrad)	2903.269	−61.431	22.856
Software algorithm (μrad)	2903.679	−62.802	20.154
Comparison error (μrad)	−0.410	1.371	2.702

The system position parameters of the four-station laser tracers in the machine tool coordinate system after calibration are shown in Table 6. The measurement results of the *X*-, *Y*-, and *Z*-axis and the comparison results with the laser tracer's built-in software are shown in Figures 6, 7 and 8, respectively. In these figures, the solid line represents the calculation result of the algorithm in this study, and the dashed line is the measurement result of the laser tracer using software. The squareness error comparison results are shown in Table 7.

It can be observed from Figure 6 that the *X*-axis geometric error calculation results from the algorithm presented this study are completely consistent with the calculation results of Etalon's own software. The linearity error EZX of the *X*-axis linear error is up to 0.9 μm; the deflection error EAX of the *X*-axis angular error is up to 1.0 μrad. The comparison results are relatively close.

It can be observed from Figure 7 that the six geometric errors of the *Y*-axis have the same trend as the results; the maximum difference of EXY is 2.0 μm, and the maximum difference of the *Y*-axis angle error is 0.5 μrad.

It can be observed from Figure 8 that the three geometric errors of the *Z*-axis exhibit exactly the same trends in the calculation results of the algorithm in this study and Etalon's software; the maximum difference of the positioning error EZZ among the *Z*-axis linear errors is 1.8 μm. The comparison results are relatively close, which illustrates the effectiveness of the algorithm.

It can be observed in Table 7 that the maximum difference between the squareness error results is the verticality E_{A0Z} between the *X*- and *Z*-axis, which is 2.7 μrad. The residuals calculated using this algorithm and the built-in algorithm of the laser tracer are compared, as shown in Figure 9.

The maximum calculated residual error for this algorithm is 2.4 μm, as shown in Figure 9(a); however, the maximum calculated residual error from the software in the Etalon laser tracer is 4.6 μm, as shown in Figure 9(b). The algorithm in this study calculates a smaller residual error; thus, it has a higher accuracy. In addition, the calculation result of the geometric error differs from that of the software because the deviation of a single result will affect the overall calculation result in addition to the base station calibration in this algorithm. Moreover, the straightness error value calculated by the software of the laser tracer does not completely restrict the end position to zero, which makes the calculation deviate. However, it can be observed that the residual error of the algorithm is smaller, and its accuracy is higher.

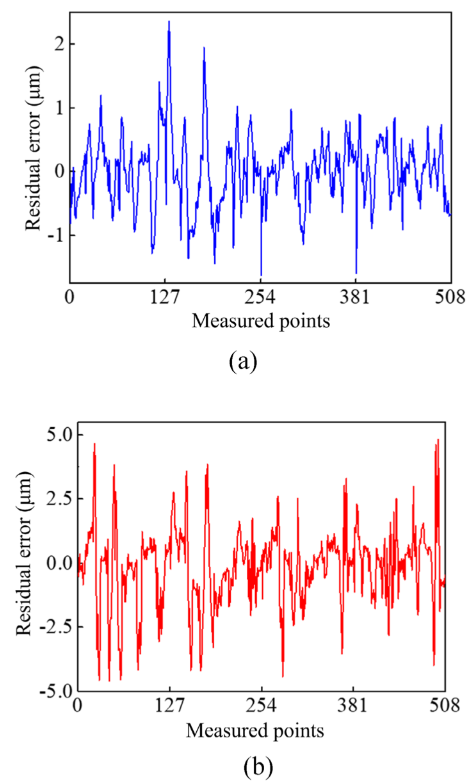

Figure 9 Residual error of various methods: (**a**) Calculated residual error of the proposal algorithm, (**b**) Calculated residual error of the Etalon algorithm

6.2 Comparison of Spatial Position Errors of CNC Machine Tools

To further verify the effectiveness of the algorithm in this study, the geometric error separation results of CNC machine tools according to the laser tracer are used to obtain the spatial position error according to the 17-term geometric error model of the three-axis CNC machine tool. The spatial position error is compared with the calculation result from the software of the laser tracer. The equation used to calculate formula for calculating the spatial position error is:

$$\boldsymbol{E} = \boldsymbol{C} \cdot \boldsymbol{P}, \tag{29}$$

where $\boldsymbol{E}$ is the spatial position error, $\boldsymbol{C}$ is the coefficient matrix, and $\boldsymbol{P}$ is the 17 geometric errors.

The spatial position error calculated according to the built-in software of the laser tracer is compared with that obtained by the algorithm in this study, as shown in Figure 10. Among these errors, delt x, delt y, and delt z are the differences between the tracker's calculation results and the *X*-, *Y*-, and *Z*-coordinates calculated by this algorithm, respectively. The approximate symmetrical difference between the X and Z spatial positions is caused by applying different weights to the X and Z solutions, which is the difference of the algorithm itself. The absolute value of the maximum spatial position error difference of the three-axis gantry structure CNC machine tool is 12.0 μm.

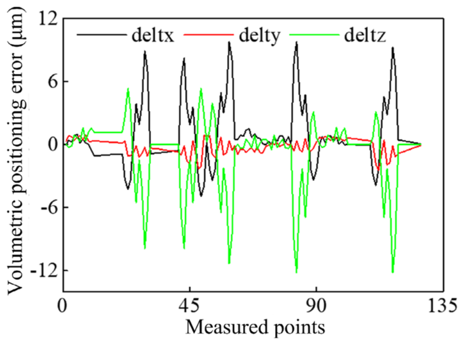

Figure 10 Comparison of volumetric positioning errors between Etalon algorithm and proposed calculation algorithm

7 Conclusions

(1) A geometric error identification method of gantry-type CNC machine tool based on multi-station synchronization laser tracers is proposed in this research. The composition of the geometric error terms of three-axis CNC machine tools is analyzed, and the geometric error model of three-axis gantry CNC machine tools is established based on screw theory.
(2) The geometric error measurement and separation algorithm of three-axis gantry CNC machine tools is derived based on the principle of multi-point positioning.
(3) The proposed method was applied to the geometric error measurement experiment of the three-axis gantry structure CNC machine tool. The results calculated by this algorithm are compared with the calculation results of the Etalon laser tracer, and they exhibit maximum linear, angular, and spatial position error differences of 2.0 μm, 2.7 μrad, and 12.0 μm, respectively, which verify the correctness of the algorithm.

Currently, the algorithm haven't applied on other types of multi-axis machine tools, like five axis machine tools integrated with rotational function parts. In the future, the algorithm versatility verification is the main focus, also includes the integration with measuring instruments.

Acknowledgements
Not applicable.

Authors' Contributions
JZ was in charge of the whole trial and wrote the manuscript; HZ assisted with sampling and laboratory analyses, building up the framework of the research. All authors read and approved the final manuscript.

Funding
Supported by Natural Science Foundation of Shaanxi Province of China (Grant No. 2021JM010), Suzhou Municipal Natural Science Foundation of China (Grant Nos. SYG202018, SYG202134).

Data availability
The datasets used and/or analysed during the current study are available from the corresponding author on reasonable request.

Declarations

Competing Interests
The authors declare no competing financial interests.

Received: 16 March 2022 Revised: 3 April 2024 Accepted: 9 April 2024
Published online: 17 May 2024

References

[1] J H Feng. Multilateration technology on the small airport surface surveillance. *Computer Simulation*, 2016, 33(7): 61−64.
[2] J R Lin, J G Zhu, Y Guo, et al. Establishment of precise three-dimensional coordinate control network in field large-space measurement. *Journal of Mechanical Engineering*, 2012, 48(4): 6−11. (in Chinese)
[3] X Y Lu. *Design and implementation of an aircraft component butt software system based on laser tracker*. Shanghai: Shanghai Jiaotong University, 2012. (in Chinese)
[4] W Wang, Y Huang, J P Zhuang. Application of laser tracker in assembly jig manufacturing for airplane. *Aeronautical Manufacturing Technology*, 2004, 12: 8184. (in Chinese)
[5] H Schwenke, R Schmitt, P Jatzkowski, et al. On-the-fly calibration of linear and rotary axes of machine tools and CMMs using a tracking interferometer. *CIRP Annals—Manufacturing Technology*, 2009, 58(1): 4773480.
[6] G Fu, J Fu, H Gao, et al. Squareness error modeling for multi-axis machine tools via synthesizing the motion of the axes. *International Journal of Advanced Manufacturing Technology*, 2017, 89(9−12): 2993−3008.
[7] J D Wang, J J Guo, Y F Deng, et al. Geometric precision detection for numerical control machine tool based on laser tracker. *Journal of Xi'an Jiaotong University*, 2011, 45(3): 85−90. (in Chinese)
[8] Z J Zhang, H Hu, X Liu. Measurement of geometric error of machine tool guideway system based on laser tracker. *Chinese Journal of Lasers*, 2011, 38(9): 159−164. (in Chinese)
[9] Z J Zhang, H Hu. Measurement of geometric error of rotary stage system based on laser tracker. *Chinese Journal of Lasers*, 2012, 39(11): 180−186. (in Chinese)
[10] H T Li, J J Guo, Y F Deng, et al. Pose Measuring principle of geometric accuracy of numerical control machine tools. *Journal of Xi'an Jiaotong University*, 2016, 50(11): 62−68. (in Chinese)
[11] M Camboulives, C Lartigue, P Bourdet, et al. Calibration of a 3D working space by multilateration. *Precision Engineering*, 2016, 44: 163−170.
[12] E Gomez-Acedo, A Olarra, M Zubieta, et al. Method for measuring thermal distortion in large machine tools by means of multilateration. *International Journal of Advanced Manufacturing Technology*, 2015, 80(1−4): 523-534.
[13] S Ibaraki, P Blaser, M Shimoike, et al. Measurement of thermal influence on a two-dimensional motion trajectory using a tracking interferometer. *CIRP Annals - Manufacturing Technology*, 2016, 65(1): 483−486.
[14] H H Lee, J G Son, S H Yang. Techniques for measuring and compensating for servo mismatch in machine tools using a laser tracker. *International Journal of Advanced Manufacturing Technology*, 2017, 92(5−8): 2919−2928.
[15] Y B Lin, G X Zhang, Z Li, et al. Self-calibration and simulation of the four-beam laser tracking interferometer system for 3D coordinate measurement. *Chinese Journal of Scientific Instrument*, 2003, 24(2): 205−210. (in Chinese)
[16] T Takatsuji. Laser-tracking interferometer system based on trilateration and a restriction on the position of its laser trackers. *Proceedings of SPIE - The International Society for Optical Engineering*, 1998, 3479.
[17] H X Song, Z Y Shi. Application and basic principle of laser tracer. *Tool Engineering*, 2015, 49(4): 85−91. (in Chinese)
[18] H Chen, Z Tan, Z Shi, et al. Optimization method for solution model of laser tracker multilateration measurement. *Measurement Science Review*, 2016, 16(4): 205−210.
[19] A Wan, L Song, J Xu, et al. Calibration and compensation of machine tool volumetric error using a laser tracker. *International Journal of Machine Tools & Manufacture*, 2018, 124: 126−133.

[20] K Wendt, H Schwenke, W Bösemann, et al. *Inspection of large CMMs by sequential multi-lateration using a single laser tracker*. Laser Metrology & Machine Performance VI, 2003.
[21] H Schwenke, M Franke, J Hannaford, et al. Error mapping of CMMs and machine tools by a single tracking interferometer. *CIRP Annals - Manufacturing Technology*, 2005, 54(1): 475−478.
[22] H T Li, J J Guo, Y F Deng, et al. Identification of geometric deviations inherent to multi-axis machine tools based on the pose measurement principle. *Measurement Science and Technology*, 2016, 27(12): 125008.
[23] J Zha, L H Li, L Han, et al. Four-station laser tracer-based geometric error measurement of rotary table. *Measurement Science and Technology*, 2020, 31: 065008
[24] J Zha, T Wang, L H Li, et al. Volumetric error compensation of machine tool using laser tracer and machining verification. The *International Journal of Advanced Manufacturing Technology*, 2020, 108: 2467–2481.
[25] Y T Wang, D Wang, S Z Zhang, et al. Design and development of a five-axis machine tool with high accuracy, stiffness and efficiency for aero-engine casing manufacturing. *Chinese Journal of Aeronautics*, 2022, 35(4): 485−496.
[26] D Wang, S Z Zhang, L P Wang, et al. Developing a ball screw drive system of high-speed machine tool considering dynamics. *IEEE Transactions on Industrial Electronics*, 2022, 69(5): 4966−4976.
[27] H L Zheng, X P Xiang, T Hu, et al. Distinct modeling and identification technology for rotary axes geometric error elements of five axis machining center. *China Mechanical Engineering*, 2021, 32(5): 547−555. (in Chinese)
[28] T Hu, W K Wang, G F Yin, et al. Screw theory based modeling methodology of horizontal machining center volumetric error and its quantitative validation. *China Mechanical Engineering*, 2020, 31(21): 2547−2556. (in Chinese)

Jun Zha born in 1987, is currently a associate researcher at *School of Mechanical Engineering, Xi'an Jiaotong University, China*. His research interests include high speed and high performance machining technology, precision components in machine tools.

Huijie Zhang born in 1982, is currently a senior engineer at *Collaborative Innovation Center, Xi'an Jiaotong University, China*. His main research interests include CNC machine tool and cutting dynamics, intelligent equipment theory and method.